Supplementary Figures

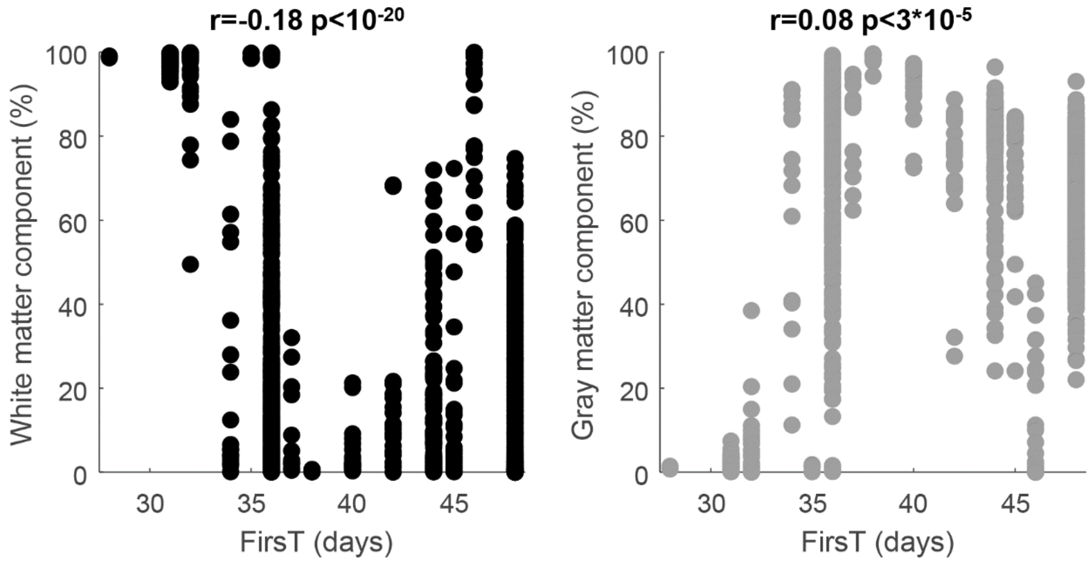

Supplementary Figure 1. Quantification of white and gray matter per ROIs. *Percent of white (left plot) and gray (right plot) matter per ROI as function of neurogenesis time.*

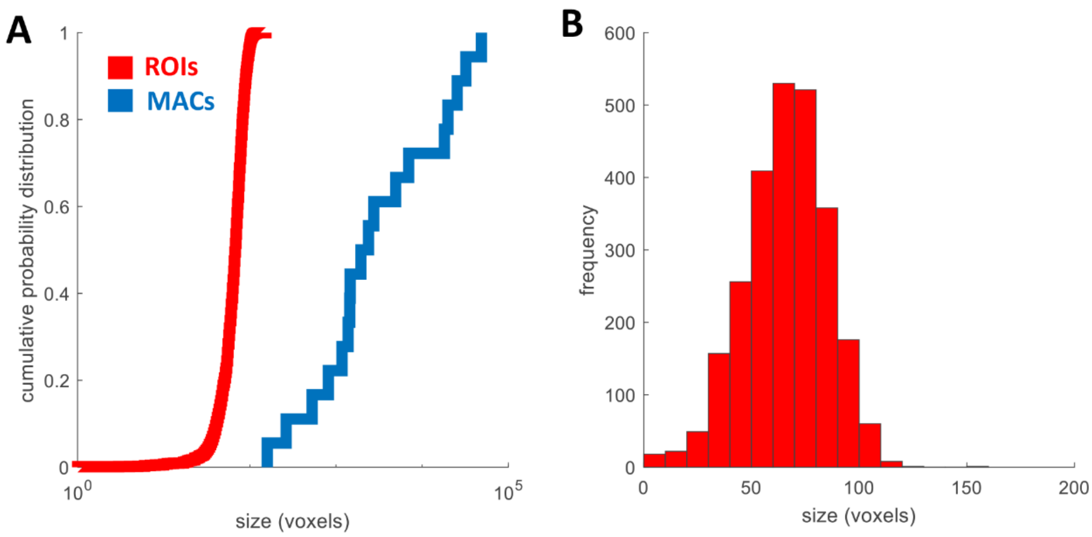

Supplementary Figure 2. Distributions of MACs and ROIs' volumes. A *distribution of ROIs volume.* ***B*** *Cumulative distribution of ROIs and MACs volumes.*

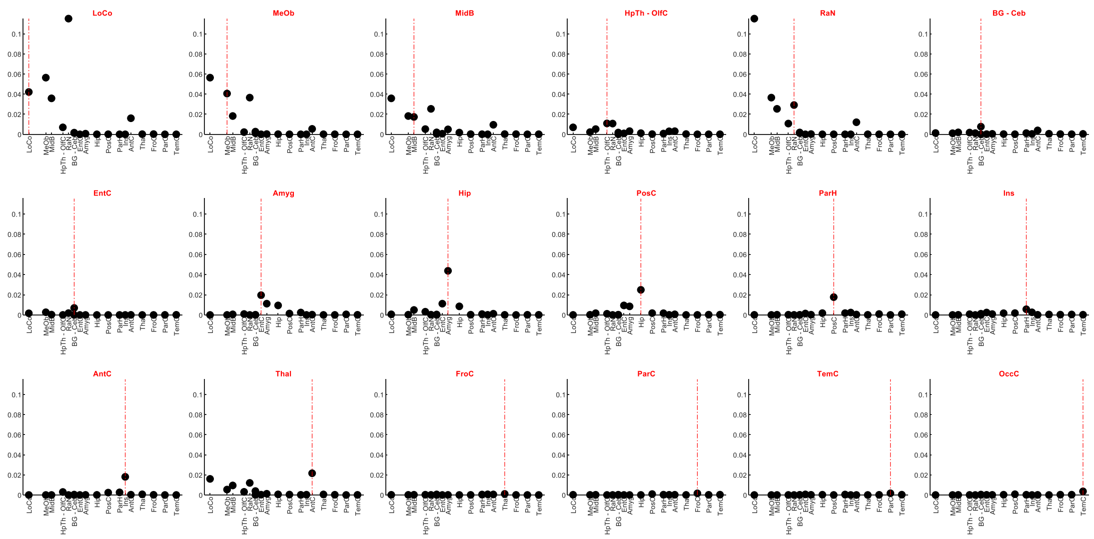

Supplementary Figure 3. **Average structural links' weight connecting ROIs belonging to different MACs (global link weight, see Methods)**. The connectivity of a given MAC (specified on the top of the scatterplot) to all other MAC (shown on the x-axis, ordered according to increasing FirsT) is plotted. The vertical broken red line marks the time point of the considered MAC. Note that the scatterplot from top left to bottom right are ordered according to increasing FirsT.

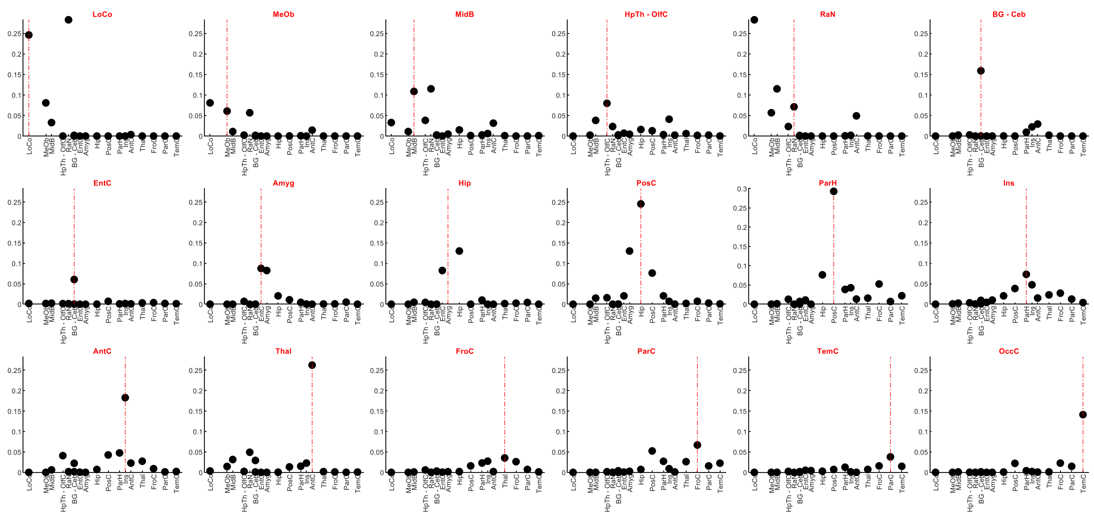

Supplementary Figure 4. **Average functional links' weight connecting ROIs belonging to different MACs (global link weight, see Methods)**. The representation is the same as described in supplementary figure 3.

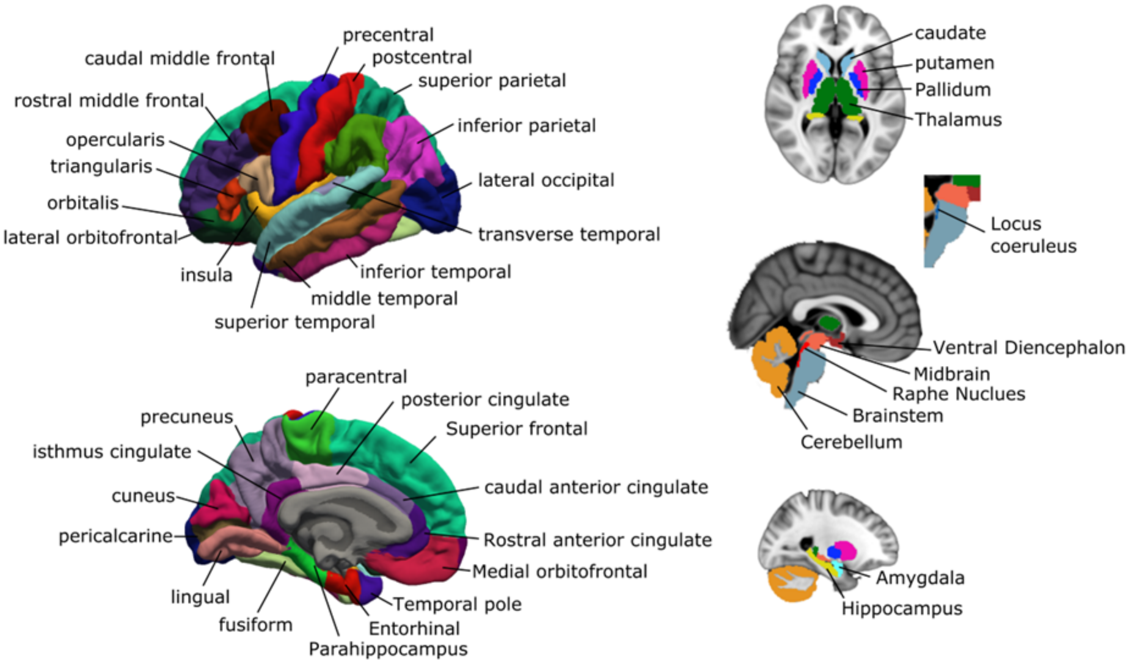

Supplementary Figure 5. **90 Regions Parcellation for Transcriptome Projection**. This custom parcellation scheme integrates multiple widely used anatomical atlases, comprising 68 cortical regions sourced from the established Desikan-Killiany atlas, 16 standard subcortical regions extracted from the FreeSurfer segmentation, and 6 specific sub-regions including the cerebellum, brainstem, locus coeruleus, and dorsal raphe nucleus.

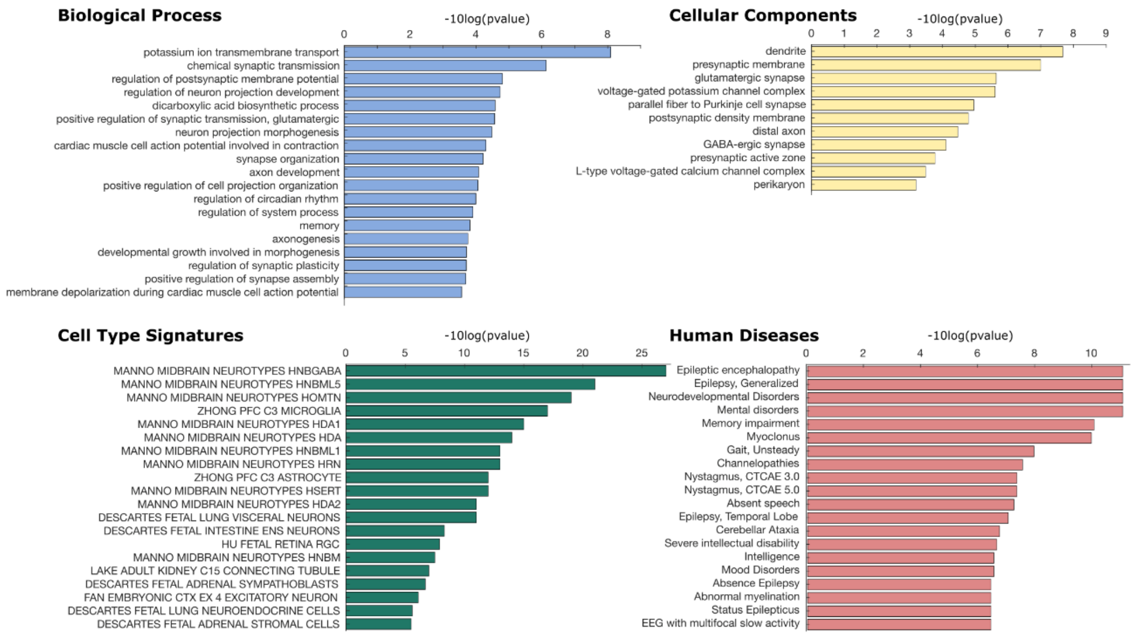

Supplementary Figure 6. Gene-set enrichment of genes with high spatial similarity with FirsT. 1,268 genes from the positive tail (6% of protein coding genes) were used to compute the overrepresentation analysis for different annotations: biological processes, cell components, cell types, and human diseases. The obtained results are similar to the ones obtained with the composite measures of FirsT and functional and structural connectivity.

MAC #	MAC name	Atlas	Reference
1	Locus coeruleus	ascending arousal system atlas	https://pubmed.ncbi.nlm.nih.gov/22592840/
2	Medulla oblongata	Freesurfer Brainstem atlas	https://pubmed.ncbi.nlm.nih.gov/25776214/
3	Midbrain	Freesurfer Brainstem atlas	https://pubmed.ncbi.nlm.nih.gov/25776214/
4	Hypothalamus & olfactory	AAL 3	https://pubmed.ncbi.nlm.nih.gov/31521825/
5	Raphe nuclei	ascending arousal system atlas	https://pubmed.ncbi.nlm.nih.gov/22592840/
6	Basal ganglia	CIT168 subcortical atlas	https://pubmed.ncbi.nlm.nih.gov/29664465/

7	cerebellum	Freesurfer Segmentation	surfer.nmr.mgh.harvard.edu
8	Entorhinal	Desikan-killiany	https://pubmed.ncbi.nlm.nih.gov/16530430/
9	Amygdala	Freesurfer Segmentation	surfer.nmr.mgh.harvard.edu
10	Hippocampus	Freesurfer Segmentation	surfer.nmr.mgh.harvard.edu
11	Posterior cingulum	Desikan-killiany	https://pubmed.ncbi.nlm.nih.gov/16530430/
12	Parahipp & insula	Desikan-killiany	https://pubmed.ncbi.nlm.nih.gov/16530430/
13	Anterior cingulate cortex	Desikan-killiany	https://pubmed.ncbi.nlm.nih.gov/16530430/
14	Thalamus	AAL 3	https://pubmed.ncbi.nlm.nih.gov/31521825/
15	Frontal Cortex	Desikan-killiany	https://pubmed.ncbi.nlm.nih.gov/16530430/
16	Parietal Cortex	Desikan-killiany	https://pubmed.ncbi.nlm.nih.gov/16530430/
17	Temporal cortex	Desikan-killiany	https://pubmed.ncbi.nlm.nih.gov/16530430/
18	Occipital cortex	Desikan-killiany	https://pubmed.ncbi.nlm.nih.gov/16530430/

Supplementary Table 1. *List of the 18 MACs, corresponding atlases used for segmentation and references. Note that in the Atlas column, same colours are used for same Atlases.*

Auxiliary Supplementary tables.

The file "gene_correlations_rank_percentiles.xlsx" is the table reporting the 20787 coding-genes with their correlation, rank and percentile in respect to structural and functional centrality, and to FirsT.

The other .xlsx files are the tables referring to GWAS genes reported for the four brain disorders considered in this research. Acronyms for diseases and file name are: EPI – epilepsy, ASD – autism spectrum disorder, PD, Parkinson's disease, AD - Alzheimer's disease, FC – functional centrality, SC – structural centrality, FirsT. The tables report the list of GWAS genes related to a given disease, with highest or lowest correlations calculated for FirsT, structural and functional centrality, specifically in the five extreme percentiles of the distributions(see fig. 5A distributions and vertical broken lines). Each *table is divided in two parts, the list of genes with highest positive (left side, horizontally highlighted in green on the top) and negative (right side, horizontally highlighted in cyan on the top) correlations. In the correlation columns (horizontally highlighted in yellow on the top), correlation values, rank of correlation (out of 20787 genes) and percentile of correlation are reported. For simplicity, rank and percentile of positively and negatively correlated genes are calculated from the corresponding extremity of the distribution. In the relevance score columns (horizontally highlighted in orange on the top) Genecards data is considered when available, and accordingly relevance score values, rank (out of the total number of genes in the Genecards list) and percentiles (out of the relevance score distribution for the genes in the Genecards list) are reported.*

Source references of table 1

T1. Altman, J. & Bayer, S. A. Development of the brain stem in the rat. I. Thymidine-radiographic study of the time of origin of neurons of the lower medulla. J. Comp. Neurol. ***194****, 1–35 (1980).*

T2. Altman, J. & Bayer, S. A. Development of the brain stem in the rat. III. Thymidine-radiographic study of the time of origin of neurons of the vestibular and auditory nuclei of the upper medulla. J. Comp. Neurol. ***194****, 877–904 (1980).*

T3. Altman, J. & Bayer, S. A. Development of the brain stem in the rat. V. Thymidine-radiographic study of the time of origin of neurons in the midbrain tegmentum. J. Comp. Neurol. ***198****, 677–716 (1981).*

T4. Steindler, D. A. & Trosko, B. K. Two types of locus coeruleus neurons born on different embryonic days in the mouse. Anat Embryol ***179****, 423–434 (1989).*

T5. Achim, K. et al. Distinct developmental origins and regulatory mechanisms for GABAergic neurons associated with dopaminergic nuclei in the ventral mesodiencephalic region. Development ***139****, 2360–2370 (2012).*

T6. Bayer, ShirleyA., Wills, KatherineV., Triarhou, LazarosC. & Ghetti, B. Time of neuron origin and gradients of neurogenesis in midbrain dopaminergic neurons in the mouse. Exp Brain Res ***105****, (1995).*

T7. Altman, J. & Bayer, S. A. Development of the diencephalon in the rat. I. Autoradiographic study of the time of origin and settling patterns of neurons of the hypothalamus. J. Comp. Neurol. ***182****, 945–971 (1978).*

T8. Altman, J. & Bayer, S. A. Development of the diencephalon in the rat. II. Correlation of the embryonic development of the hypothalamus with the time of origin of its neurons. J. Comp. Neurol. ***182****, 973–993 (1978).*

T9. van Eerdenburg, F. J. C. M. & Rakic, P. Early neurogenesis in the anterior hypothalamus of the rhesus monkey. Developmental Brain Research ***79****, 290–296 (1994).*

T10. Workman, A. D., Charvet, C. J., Clancy, B., Darlington, R. B. & Finlay, B. L. Modeling Transformations of Neurodevelopmental Sequences across Mammalian Species. Journal of Neuroscience ***33****, 7368–7383 (2013).*

T11. Brand, S. & Rakic, P. Neurogenesis of the nucleus accumbens septi and neighboring septal nuclei in the rhesus monkey: A combined [3H]thymidine and electron microscopic study. Neuroscience ***5****, 2125–2138 (1980).*

T12. Miale, I. L. & Sidman, R. L. An autoradiographic analysis of histogenesis in the mouse cerebellum. Experimental Neurology ***4****, 277–296 (1961).*

T13. Altman, J. & Bayer, S. A. Development of the diencephalon in the rat. III. Ontogeny of the specialized ventricular linings of the hypothalamic third ventricle. J. Comp. Neurol. ***182****, 995–1015 (1978).*

T14. Leto, K., Carletti, B., Williams, I. M., Magrassi, L. & Rossi, F. Different Types of Cerebellar GABAergic Interneurons Originate from a Common Pool of Multipotent Progenitor Cells. Journal of Neuroscience ***26****, 11682–11694 (2006).*

T15. Bayer, S. A. Development of the hippocampal region in the rat I. Neurogenesis examined with3H-thymidine autoradiography. J. Comp. Neurol. ***190****, 87–114 (1980).*

*T16. McConnell, J. & Angevine, J. B. Time of neuron origin in the amygdaloid complex of the mouse. Brain Research **272**, 150–156 (1983).*

*T17. Soma, M. et al. Development of the mouse amygdala as revealed by enhanced green fluorescent protein gene transfer by means of in utero electroporation. J. Comp. Neurol. **513**, 113–128 (2009).*

*T18. Bayer, S. A. Neurogenesis in the rat primary olfactory cortex. International Journal of Developmental Neuroscience **4**, 251–271 (1986).*

*T19. Granger, B., Tekaia, F., Le Sourd, A. M., Rakic, P. & Bourgeois, J.-P. Tempo of neurogenesis and synaptogenesis in the primate cingulate mesocortex: Comparison with the neocortex. J. Comp. Neurol. **360**, 363–376 (1995).*

*T20. Altman, J. & Bayer, S. A. Development of the diencephalon in the rat. IV. Quantitative study of the time of origin of neurons and the internuclear chronological gradients in the thalamus. J. Comp. Neurol. **188**, 455–471 (1979).*

*T21. Rakic, P. Pre- and post-developmental neurogenesis in primates. Clinical Neuroscience Research **2**, 29–39 (2002).*

*T22. Reillo, I. & Borrell, V. Germinal Zones in the Developing Cerebral Cortex of Ferret: Ontogeny, Cell Cycle Kinetics, and Diversity of Progenitors. Cerebral Cortex **22**, 2039–2054 (2012).*

*T23. Charvet, C. J. Distinct developmental growth patterns account for the disproportionate expansion of the rostral and caudal isocortex in evolution. Front. Hum. Neurosci. **8**, (2014).*